URSI GASS 2020, Rome, Italy, 29 August - 5 September 2020

The response of optical emission on heating of the ionosphere by powerful radio wave

J. Legostaeva, A. Shindin, and S. Grach
Lobachevsky University, Nizhny Novgorod, 603105, http://www.unn.ru

Abstract

Numerical modeling of ionospheric heating by powerful HF radio wave's influence on the nighttime airglow and comparison of the results with experimental data obtained at the SURA heating facility are presented. We model the effect of suppression of the background airglow during the heating as well as its recovery and "afterglow" after the heating switching off. Results obtained allow to estimate the increase of electron temperature and rates of some photo-chemical reactions in the heated ionosphere.

1 Introduction

It is known that optical emission of atomic oxygen (state O^1D, 630 nm, red line) of the ionosphere modified by powerful HF radio waves exhibits two opposite effects. The first one is the enhancement of the emission intensity (artificial optical emission or artificial aurora) due to increasing collisional excitation of O^1D caused by electron acceleration by parametrically excited plasma waves. The second effect is a suppression of the background emission due to slowing down of the dissociative recombination of $O_2$with increasing electron temperature $\alpha(T_e) \propto T_e^{-1/2}$, α is the recombination coefficient[1-4].

The main purpose of the work is numerical simulations of the second effect, namely, the dynamics of the ionosphere red line emission (630 nm, transition $O^1D \rightarrow O^3P_2$) caused by powerful radio wave switching on and off and comparing the simulation results with experimental data obtained at the SURA heating facility.

Below, in the section 2, we briefly present the experimental data. The section 3 describes the theoretical model. In section 4 we discuss results obtained and compare them with the experiment.

2 Experimental data

Figures 1-4 display experimental results of studying influence of powerful HF radio waves on the red line optical emission of the ionosphere obtained at the SURA facility on September 14, 2012. SURA facility radiated vertically at the frequency 5.33 MHz with a schedule 150 s on, 270 s off. The effective radiated power was $P_{ef} \sim$ 200 MW. The night-sky images presented in Figs 1 and 3 were obtained with CCD camera S1C/079-FP(FU) with 20.6° field of view.

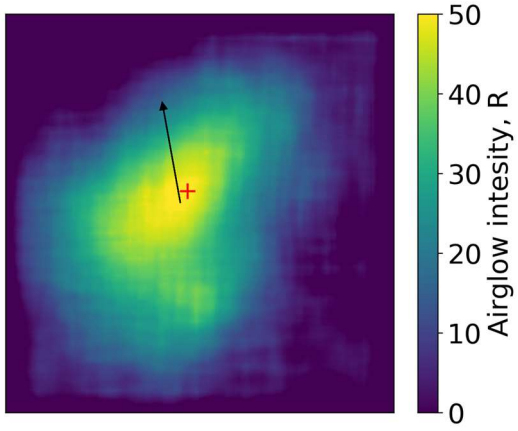

Figure 1. Night sky image in the atomic oxygen red line (630 nm) with HF pump induced emission enhancement. The exposure time is 15 s. SURA Facility, 14.09.2012, 18:09 UTC. The arrow shows the direction to geographical North.

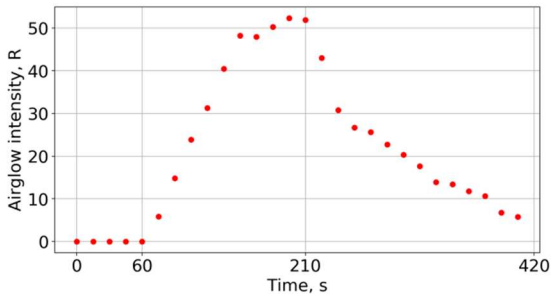

Figure 2. The 630 nm airglow intensity dynamics measured on the ground during 18:06 – 18:13 UTS 14.09.2012. t = 60 s corresponds to the pump wave switching on, t = 210 s to the pump wave switching off.

Figure 1 presents the image obtained at 22:09 local summer time (18:09 UTC+4 h), the heating session started at 18:07 UTC. It is well seen a noticeable enhancement of the emission brightness, the maximum brightness achieved 50 R. Figure 2 shows the brightness dynamics (t = 60 s corresponds to the pump wave switching on, t = 210 s to the pump wave switching off) at the point with maximum brightness across the camera field of view shown by red cross in the Figure 1. It is seen that in ~ 25 s after heating switch off the decay of the airglow brightness slows down.

In some sessions even an increase in brightness is observed in this time [2,3], we call this "afterglow".
Figures 3 and 4 illustrate the opposite effect of suppressing emission background recorded in the next heating session at 18:13 UTC. In this session performed at the pump wave frequency 5330 kHz the suppression reaches 10 R already in ~ 50 s after pump wave switching on.

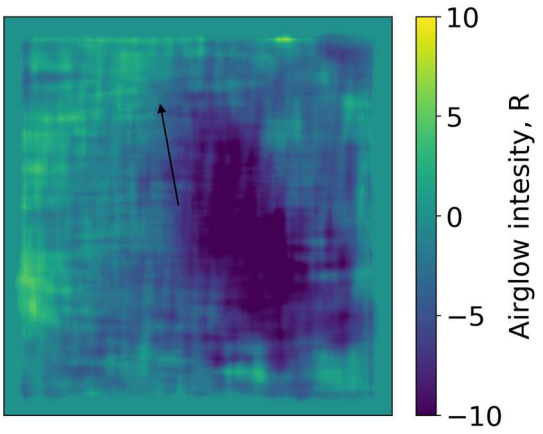

Figure 3. The same as in Fig. 1 but for 18:13:46.

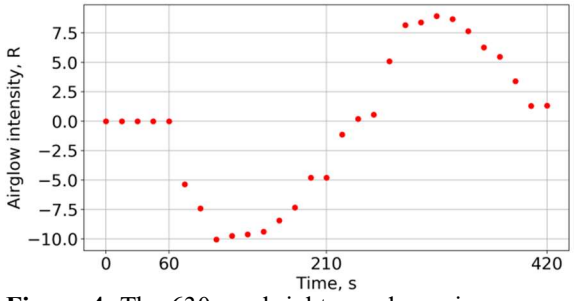

Figure 4. The 630 nm brightness dynamics measured on the ground during 18:12 – 18:19 UTS 14.09.2012

Then the emission intensity starts to recover. The recovery continues after heating switching off till t=310-320 s, and then slowly decays. During 240 s<t<420 s the airglow brightness exceeds the stationary background level without heating (afterglow). The latter effect, namely, the suppression of the background due to ionosphere heating and the successive afterglow, we try to model in this paper.

3 Theoretical model

The red line airglow measured in the experiment is determined as the integral over the entire range of heights where excited atoms O^1D exist:

$$B = A_{6300} \int [O^1D]\, dz,$$

where $A_{6300} = 7{,}1 \cdot 10^{-3}$ is the Einstein coefficient, $[O^1D]$ is the concentration of excited atoms. The brightness value is measured in Rayleigh (R), $1\,R$ = 10^6 photons/(cm^2·s) = 10^{10} photons/(m^2·s). Under natural conditions (in the absence of the HF heating), the maximum of $[O^1D] \sim 1200$ cm^{-3} is reached at altitudes 230-250 km. At these altitudes, excited atoms in the O^1D state appear as a result of a sequence of charge exchange reaction ($O^+ + O_2 \rightarrow O_2^+ + O$) and dissociative recombination of electrons with molecular oxygen ions ($O_2^+ + e^- \rightarrow O + O(^1D)$). O, O_2, O^+, O_2^+ are atomic and molecular oxygen and the corresponding ions. […] denote concentration of corresponding species.
The system of differential equations describing the dynamics of $[O_2^+]$ and $[O^1D]$ under these reactions with account of the electron heating, takes the form:

$$\frac{d[O_2^+]}{dt} = k_1[O^+][O_2] - \alpha[O_2^+]N_e \qquad (1)$$

$$\frac{d[O^1D]}{dt} = \eta\alpha[O_2^+]N_e - \frac{1}{\tau_{\text{eff}}}[O^1D], \qquad (2)$$

$$\frac{\partial T_e}{\partial t} - D_T \frac{\partial^2 T_e}{\partial z^2} + \delta\nu_e(T_e - T_0) = Q_T. \quad (3)$$

Here $k_1 = 2 \cdot 10^{-11} \frac{cm^3}{s}$ is the rate coefficient of the charge exchange reaction, α is the coefficient of dissociative recombination, $\alpha(T_e) = \alpha_0\sqrt{\frac{T_0}{T_e}}$, $\alpha_0 = 1{,}9 \cdot 10^{-7}\sqrt{\frac{300}{T_0}}$, T_0 =1000 °K is electron temperature at the powerful wave turning on (beginning of heating), N_e is the electron concentration, η = 1.1 is the probability coefficient, τ_{eff} is the effective lifetime of the atom in the state O^1D.
For calculations, we used a value of the effective electron lifetime at the O^1D level τ_{eff}, different from the radiation lifetime τ_r = 107 s. In calculating τ_{eff} the decrease in the concentration of the excited atoms in the O^1D state as a result of deactivation in collisions with nitrogen and oxygen molecules N_2, O_2 is taken into account. According to [5], under ionospheric conditions at the studied altitudes $\tau_{eff} \sim 35$ s.
Equation (3) is the electron thermal conductivity equation with the source $Q_T(z,t)$ situated near z_0, the upper hybrid resonance height of powerful radio wave related to the electron heating by the pump (electromagnetic) wave and parametrically excited plasma waves.

$$Q_T(z,t) = Q_T(z) = \frac{2E_0^2}{3N_e}\frac{\nu_e}{4\pi}\epsilon\left[h\left(z - \left[z_0 - \frac{\Delta z}{2}\right]\right) - h\left(z - \left[z_0 + \frac{\Delta z}{2}\right]\right)\right]\left[h(t - t_{on}) - h(t - t_{off})\right].$$

The initial condition for Eq. (3) is $T_e(z, t = 0) = T_0$. $h(z)$ is the Heaviside function, z is the height, z_0, the upper hybrid resonance height, is the height of the center of the heating source, $\Delta z = 1km$ is the characteristic width of the heating source, t_{on} and t_{off} are the times of turning on and off the powerful wave, respectively, $D_T = l_e v_e^2$, $l_e = 600m$ is the mean free path, $\delta = 10^{-4}$ is the fraction of energy lost by the electron during collision with

heavy particle, m_e is the mass of the electron and ν_e = 300 s^{-1} is the electron collision frequency, E_0^2 is the intensity of the pump wave electric field. For calculations, we use for E_0 the formula $E_o(z)[V/m] = 9.5\frac{\sqrt{W_0[kW]}}{z(m)}$, where $W_0 = 175\ kW$ is the power of the transmitter pumping the ionosphere. $\epsilon >> 1$ is coefficient enlarging the source due to inclusion of plasma waves in heating process.

Based on the solution of equations (1) - (3), the height distribution of concentrations [O_2] and [O], taken from the empirical model of the atmosphere NRLMSISE-00 [6], and the electron concentration profile N_e, taken from the International Reference Ionosphere model (IRI) [7] and modified taking into account the conditions of the experiment, a behavior of the concentration [O^1D] and the brightness of the optical glow in the ionospheric experiments performed at the SURA facility was modeled. Examples of simulation results are shown in Figures 5 and 6 (blue lines). Figure 5 displays the distribution of [O^1D] for the heating source position z_0=270 *km* after subtraction of the background. Figure 6 exhibits the emission brightness dynamics on the ground for two different sets of the of simulation parameters: the same as in Fig. 5 (dashed line) and (solid line) slightly varied for better coincidence with experimental data (red dots taken from Fig. 4).

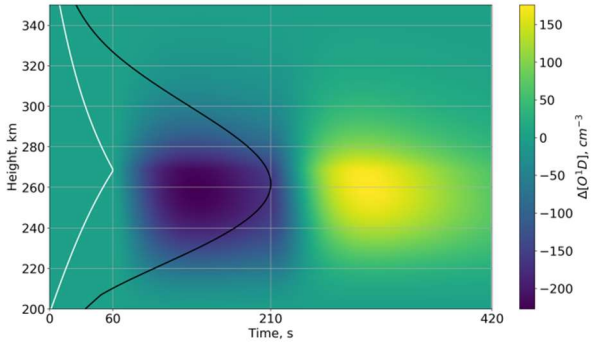

Figure 5. Simulations of heating-induced excited oxygen O^1D concentration *vs.* time for the session 18:07 – 18:13 UTS. Black and white lines illustrate height distribution of [O^1D] without heating and the electron temperature T_e height distribution before heating switching off. The maximum of [O^1D] is 1200 cm^{-3}, T_e maximum is 800 K.

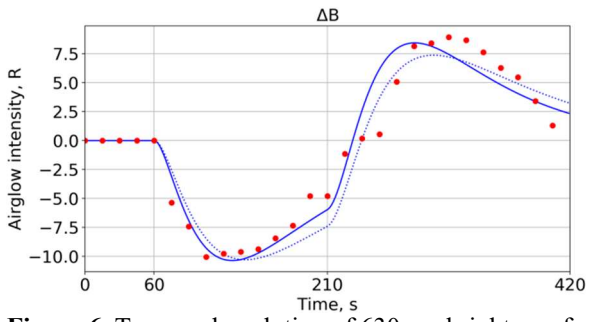

Figure 6. Temporal evolution of 630 nm brightness for the session 18:07 – 18:13 UTS. t = 60 s corresponds to the pump wave switching on, t = 210 s to the pump wave switching off. Red dots present the experimental data taken from Fig.4, dashed line corresponds to the modeling with parameters shown the Section 3 with $\epsilon = 15$. For solid line the following parameters were taken: $\epsilon = 20$, $\alpha(Te)$=1.5$\alpha_0(T_0/T_e)^{1/2}$.

4 Discussion

A suppression of the 630 nm optical emission was observed in the experiments at the SURA facility in 2010 -2016 in a number of sessions with heating of the ionosphere by powerful electromagnetic wave of ordinary polarization [3,4]. Previously, similar, but weaker effect was observed at Platteville and Arecibo facilities with heating by extraordinary polarized powerful wave [1]. For ordinary polarization this effect was, most probably, masked by the opposite one: an increase of the emission brightness caused by oxygen atoms collisions with electrons accelerated by parametrically excited plasma waves. The effect caused by ordinary pump wave is stronger than for extraordinary one and is accompanied with an increase of the emission intensity after turning off the heating (afterglow).

Using the theoretical model which includes the equations for charge exchange reaction, dissociative recombination and electron thermal conductivity (1)-(3) we tried to combine the simulation results with experimental data.

From Figs. 5, 6 it is seen that temporal behavior of the measured emission brightness is qualitatively similar to one obtained from simulations.

The suppression of the emission intensity is determined, as already mentioned, by a decrease in the coefficient of dissociative recombination α with increasing electron temperature, a decrease in [O^1D] in accordance with equation (2), and, consequently, the brightness of optical emission B. When the pump wave is turned off, the electrons cool down, T_e decreases, α and, therefore, [O^1D] increase, which leads to a temporary increase in brightness (afterglow). The characteristic times of brightness variations during simulation is determined by the reaction coefficients and, as we see, are close to the experimentally observed ones. With some, perhaps arbitrary, variations of the simulation parameters, it is possible practically to combine the theoretical curve with the experimental points. Variations of parameters are given in the captions to Figures 5, 6.

Notice that for the long heating (t > 150 s in our case) the stationary ($\frac{\partial}{\partial t} = 0$) brightness value B equal to the initial one (B=0 in the Fig. 6) should be achieved. The same brightness should be attained after the heating switching off and temporary brightness increase (afterglow).

Thus, modeling the effect of electron heating on the behavior of the glow in the 630 nm line may be useful for estimating a number of ionosphere parameters. In particular, there are a concentration of excited oxygen atoms and its variations during and after heating, the height of the glow source in the red line, the magnitude of the electron temperature increase under heating, the reaction coefficients responsible for the brightness dynamics.

At the same time, it remains unclear why in some successive heating sessions very close in time, an abrupt

change in the observed effect can happen: a brightness growth in a compact spot with its suppression in a sufficiently wide region is replaces by heating sessions when the electron acceleration does not exist or is very weak, and the suppression of the airglow prevails and is observed.

In [2,3] it was shown that the suppression effect occurred when the pump wave frequency approaches the critical frequency of the ionosphere as a result of the after sunset drop of the ionosphere. Apparently, in the experiment presented in this work, there was a short-term (within one session) approaching of the pump wave frequency to the 4^{th} electron gyroharmonic due to altitude variations of the ionosphere.

5 Acknowledgements

The work is supported by RFBR grants 18-02-00622 and 20-32-70198.

References

1. Grach S.M., Sergeev E.N., Mishin E.V., Shindin A.V., Dynamic properties of ionospheric plasma turbulence driven by high-power high-frequency radiowaves, Physics Uspekhi 59 (11) 1091 ± 1128 (2016), doi: https://doi.org/10.3367/UFNe.2016.07.037868

2. Klimenko V.V., Grach S.M., Sergeev E.N., Shindin A.V., Features of the ionospheric artificial airglow caused by OHMIC heating and plasma turbulence-accelerated electrons induced by HF pumping of the SURA heating facility, Radiophysics and Quantum Electronics, 60 (6), (2017), doi: 10.1007/s11141-017-9812-0

3. Grach S.M., Klimenko V.V., Shindin A.V., Nasyrov I.A., Sergeev E.N., Yashnov V.A., Pogorelko N.A., Airglow during ionospheric modifications by the SURA facility radiation. Radiophysics and Quantum Electronics, 55 (1–2), (2012).

4. Sipler D.P., Biondi M.A., J.Geophys.Res. 83(A4), 1519-1522 (1978).

5. Link and Cogger, JGR, 93 (A9), 9883-9892, (1988).

6. Picone, J. M., A. E. Hedin, D. P. Drob, and A. C. Aikin. //NRLMSISE-00 Empirical model of the atmosphere: Statistical comparisons and scientific issues, JGR, 107(A12), 1468, doi: 10.1029/2002JA009430, (2002).

7. https://ccmc.gsfc.nasa.gov/modelweb/models/iri-vitmo.php